Single-cell RNA-seq identifies a reversible mesodermal activation in abnormally specified epithelia of p63 EEC syndrome

Eduardo Soares[a,b,1], Quan Xu[a,1], Qingqing Li[c,d,1], Jieqiong Qu[a], Yuxuan Zheng[c,d,e], Henriette H. M. Raeven[a], Karina O. Brandao[a], Isabelle Petit[f,g], Willem M. R. van den Akker[a], Simon J. van Heeringen[a], Daniel Aberdam[f,g], Fuchou Tang[c,d,e,2], and Huiqing Zhou[a,h,2]

[a]Department of Molecular Developmental Biology, Faculty of Science, Radboud Institute for Molecular Life Sciences, Radboud University, 6525GA Nijmegen, The Netherlands; [b]Coordenação de Aperfeiçoamento de Pessoal de Nível Superior (CAPES) Foundation, Ministry of Education of Brazil, 70.040-031 Brasília, Brazil; [c]Beijing Advanced Innovation Center for Genomics, Ministry of Education Key Laboratory of Cell Proliferation and Differentiation, College of Life Sciences, Peking University, 100871 Beijing, China; [d]Biomedical Pioneering Innovation Center, Peking University, 100871 Beijing, China; [e]Peking-Tsinghua Center for Life Sciences, Peking University, 100871 Beijing, China; [f]Hôpital Saint-Louis, Université de Paris, U976, INSERM, F-75010 Paris, France; [g]Skin, Stem & Development Lab, Université de Paris, F-75010 Paris, France; and [h]Department of Human Genetics, Radboud Institute for Molecular Life Sciences, Radboud University Medical Center, 6525GA Nijmegen, The Netherlands

Edited by Joan S. Brugge, Harvard Medical School, Boston, MA, and approved July 15, 2019 (received for review May 23, 2019)

Mutations in transcription factor p63 are associated with developmental disorders that manifest defects in stratified epithelia including the epidermis. The underlying cellular and molecular mechanism is however not yet understood. We established an epidermal commitment model using human induced pluripotent stem cells (iPSCs) and characterized differentiation defects of iPSCs derived from ectrodactyly, ectodermal dysplasia, and cleft lip/palate (EEC) syndrome patients carrying p63 mutations. Transcriptome analyses revealed stepwise cell fate transitions during epidermal commitment: Specification from multipotent simple epithelium to basal stratified epithelia and ultimately to the mature epidermal fate. Differentiation defects of EEC iPSCs caused by p63 mutations occurred during the specification switch from the simple epithelium to the basal-stratified epithelial fate. Single-cell transcriptome and pseudotime analyses of cell states identified mesodermal activation that was associated with the deviated commitment route of EEC iPSCs. Integrated analyses of differentially regulated genes and p63-dependent dynamic genomic enhancers during epidermal commitment suggest that p63 directly controls epidermal gene activation at the specification switch and has an indirect effect on mesodermal gene repression. Importantly, inhibitors of mesodermal induction enhanced epidermal commitment of EEC iPSCs. Our findings demonstrate that p63 is required for specification of stratified epithelia, and that epidermal commitment defects caused by p63 mutations can be reversed by repressing mesodermal induction. This study provides insights into disease mechanisms underlying stratified epithelial defects caused by p63 mutations and suggests potential therapeutic strategies for the disease.

p63 | single-cell RNA-seq | stratified epithelia | EEC | cell fate commitment

The transcription factor p63 is a key regulator in development of stratified epithelia in many organs (1–3). Deletion of p63 in mice results in striking developmental defects or even complete absence of stratified epithelia in organs such as the epidermis (2–5). In humans, heterozygous mutations in *TP63* encoding the p63 protein give rise to several autosomal dominant developmental disorders (6). These disorders manifest defects in tissues and organs where stratified epithelia are present, and their phenotypes resemble those in p63 knockout mice (2, 3), although in milder forms. One of these disorders is ectrodactyly, ectodermal dysplasia, and cleft lip/palate (EEC) syndrome (OMIM 604292) that is associated with mutations located in the p63 DNA-binding domain (7). EEC patients exhibit all of the characteristic phenotypes of p63 mutation-associated diseases, namely, defects in the epidermis and epidermal-related appendages, limb malformation, and orofacial clefting. Hotspot mutations in the p63 DNA-binding domain affecting amino acids such as R204 and R304 have been reported to account for ∼90% of the EEC cases (8). Consistent with the dominant inheritance pattern, these mutations have been shown to have a dominant negative effect by abolishing p63 DNA binding (7). How p63 EEC mutations affect development of stratified epithelia at the cellular and molecular level is however not yet fully understood.

The epidermis is probably the best studied model for p63 function. It has been established that p63 plays a pivotal role in epidermal keratinocytes (KCs) and orchestrates essential cellular programs, including stem cell maintenance and proliferation, differentiation, and adhesion (9–11). In 2 different p63 knockout mouse models, epidermal defects have been consistently reported (2–5), even though 1 of the models was later shown to be

Significance

Mutations in p63 cause several developmental disorders with defects of epithelial-related organs and tissues, including the epidermis. Our study dissects the unknown cellular and molecular pathomechanism. We utilized human induced pluripotent stem cells (iPSCs) derived from ectrodactyly, ectodermal dysplasia, and cleft lip/palate (EEC) syndrome patients carrying p63 mutations, and studied transcriptomic and genomic changes during differentiation of these cells to epidermal cells. Our analyses showed that specification of the proper epithelial cell state was affected by p63 EEC mutations, with abnormal mesodermal activation. Inhibitors of mesodermal induction enhanced epidermal commitment. This study provides insights into disease mechanisms associated with p63 mutations and suggests potential therapeutic strategies.

Author contributions: E.S., Q.X., Q.L., F.T., and H.Z. designed research; E.S., Q.L., J.Q., H.H.M.R., K.O.B., W.M.R.v.d.A., and H.Z. performed research; I.P., S.J.v.H., and D.A. contributed new reagents/analytic tools; E.S., Q.X., Y.Z., and H.Z. analyzed data; and E.S., Q.X., Q.L., F.T., and H.Z. wrote the paper.

The authors declare no conflict of interest.

This article is a PNAS Direct Submission.

Data deposition: The data of anonymous controls reported in this paper have been deposited in the Gene Expression Omnibus (GEO) database, https://www.ncbi.nlm.nih.gov/geo (accession no. GSE120107). Data of p63 patients have been deposited in the Genotypes and Phenotypes (dbGaP) database (accession no. phs001737.v2.p1).

[1]E.S., Q.X., and Q.L. contributed equally to this work.

[2]To whom correspondence may be addressed. Email: tangfuchou@pku.edu.cn or j.zhou@science.ru.nl.

This article contains supporting information online at www.pnas.org/lookup/suppl/doi:10.1073/pnas.1908180116/-/DCSupplemental.

Published online August 14, 2019.

hypomorphic (12). It has also been shown that the epithelial fate is compromised in p63-deficient epidermal cells (13). Although p63 has undoubted importance in epithelial cells, the cellular function of p63 during epidermal development is still under debate. One model suggests that p63 is not required for commitment toward the epidermal fate, as a small number of cells expressed epidermal marker genes Krt5 and Krt14, and the morphology of cells and tissues was relatively normal in p63 knockout mice (5). Other studies reported that cells and tissues in p63 knockout mice retained Krt8 and Krt18 expression that marked the ectodermal rather than the epidermal fate, concomitant with induced mesodermal genes (14). These findings support a model in which p63 is essential for epidermal commitment and acts as a gatekeeper of the epithelial lineage (14). One explanation for these opposite interpretations is probably because observations were made based on a limited panel of marker genes or from a small number of cells in a heterogeneous population. The analysis of the complete transcriptome, especially the single-cell transcriptome that captures heterogeneous cell states (15, 16), may resolve this issue.

Human induced pluripotent stem cells (iPSCs) have provided revolutionary tools for disease modeling and for testing potential therapeutic compounds using relevant patient material (17). In this study, we derived epidermal KCs from human iPSCs of healthy controls and EEC patients carrying a p63 mutation, R204W or R304W (18). Bulk and single-cell RNA-seq were performed to examine cell states using an in vitro epidermal commitment model. The time course RNA-seq analysis during epidermal commitment of control iPSCs showed that the initial iPSCs entered an intermediate "multipotent" phase before switching and committing toward the basal stratified epithelial fate, followed by a maturation phase specific for the epidermal fate. Importantly, EEC iPSCs largely failed to make the switch toward the epithelial fate and showed enhanced nonepithelial cell identity. Epidermal commitment of EEC iPSCs was enhanced by inhibitors of mesodermal induction. It should be noted that 1 of the N-terminal isoforms, ΔNp63, is predominantly expressed and shown to be essential in epidermal cells (1, 10, 13). Our findings may therefore be most relevant to the biology of the ΔNp63 isoform.

Results

Generation of Functional Induced Keratinocytes (iKCs) from iPSCs. To obtain robust epidermal commitment readouts, we used control iPSCs derived from 2 different individuals, generated from dermal fibroblasts donated by healthy individuals. One commonly used human embryonic stem cell line (ESC-H9) (19) was also used in parallel as the control. Pluripotency and the differentiation capacity of the 2 iPSC lines were confirmed by the expression of pluripotency marker genes, OCT4 and SSEA4, and the in vitro differentiation assay to 3 germ layers (*SI Appendix*, Fig. S1). All 3 lines together are termed pluripotent stem cells (PSCs). To facilitate transcriptome studies, we established a complete feeder-free workflow (Fig. 1*A*) by modifying a 30-d differentiation protocol of combining retinoic acid (RA) for inducing the ectodermal fate and bone morphogenetic protein 4 (BMP4) for repressing the neuronal fate (20). Using this workflow, we directed the 3 control PSC lines toward the epidermal fate and examined the differentiation process at days 0, 4, 7, 15, and 30. The morphology of differentiating PSCs started to change on day 4 into a cobblestone shape that was similar to that of keratinocytes (Fig. 1*A*). The basal epidermal markers p63 and KRT14 were induced weakly on day 4, became more visible on day 7, and were then progressively up-regulated till day 30 in iKCs (Fig. 1 *B* and *C*). Epidermal commitment of these PSCs was also confirmed by marker gene expression at the mRNA level, namely down-regulated pluripotency marker *OCT4*, firstly induced and subsequently decreased simple epithelial markers *KRT8* and *KRT18*, and up-regulated *TP63* and *KRT14* (Fig. 1*D*). To assess whether the PSC-derived iKCs harbored stratification potential, we induced terminal differentiation of iKCs by including serum in the 2D culture medium. Upon induction for 72 h, induced expression of terminal differentiation markers, transglutaminase I (*TGM1*), involucrin (*IVL*), and cysteine protease inhibitor cystatin M/E (*CYSME*), was detected (*SI Appendix*, Fig. S2 *A* and *B*). These data indicated that these iKCs behave similarly to epidermal KC that can stratify. Taken together, iKCs derived from PSCs displayed both morphological and functional properties of epidermal KCs.

To characterize the epidermal commitment process, we performed time-course RNA-seq analyses of differentiating PSC cells, and compared them with that of primary epidermal KCs (Dataset S1). K-means clustering analysis of the top 500 differentially expressed (DE) genes during differentiation identified 6 distinct clusters (Fig. 1*E*, *SI Appendix*, Fig. S2*E*, and Dataset S2). Cluster 1 (e.g., *NANOG*) and cluster 2 (e.g., *SOX2*) were highly expressed in PSCs, and contained genes involved in stem cell maintenance and early embryonic morphogenesis based on gene ontology (GO) analysis. Genes in cluster 3 such as *MSX1* were transiently induced and subsequently switched off and are involved in embryonic development (reproduction) and cell proliferation. Genes in cluster 4, e.g., *IGFBP3*, were induced during early epidermal differentiation and stayed at a high level until differentiation day 30. Many of these genes play roles in cell migration and adhesion, embryonic morphogenesis, and development of different organs. Importantly, cluster 5 included genes such as *KRT5* and *TP63* that are involved in epithelial and epidermal development, desmosome assembly, and extracellular matrix organization. These genes were lowly expressed or not expressed in PSCs and during early differentiation and significantly induced on day 15 and remained high on day 30. The expression levels of these genes were similar to their expression in KCs. Remarkably, ΔNp63 was the only induced and expressed p63 isoform that was detected in our RNA-seq data (*SI Appendix*, Fig. S2*I*) and quantitative RT-PCR (qRT-PCR) analyses during PSC differentiation (Fig. 1*D*). This is consistent with the previously reported role of this p63 isoform in epidermal development (1, 10, 13). Interestingly, cluster 6 also contained epidermal genes such as *KRT14*, *IVL*, and *FLG* that play roles in keratinocyte differentiation and barrier formation, although they remained lowly expressed in day-30 iKCs as compared to primary KCs. The gene expression during differentiation was also shown by principal component analysis (PCA), indicating that PSCs went through distinct phases during epidermal commitment (*SI Appendix*, Fig. S2 *C* and *D* and Dataset S3).

Our RNA-seq analyses revealed different phases of gene expression during epidermal differentiation; for example, cluster 2 and cluster 3 genes were induced at a high level at an early differentiation stage (days 4 and 7) and subsequently turned off, and cluster 5 and 6 genes were expressed at the end of epidermal differentiation (day 30) or in epidermal keratinocytes. This dynamic gene expression pattern probably represents a switch from a multipotent state to the epidermal fate during development. To interrogate whether the dynamic gene expression pattern observed in our in vitro cellular model recapitulates in vivo epidermal development, we examined RNA-seq data obtained from the mouse embryonic epidermis (21). Cluster 2 and 3 genes indeed showed a higher level of expression in the E9 mouse embryonic skin, whereas cluster 5 and 6 genes had a higher expression in E13 mouse embryonic skin (Fig. 1*F*). These findings demonstrate that the gene expression pattern obtained from PSC epidermal differentiation is consistent with that during epidermal development in vivo.

p63 Predominantly Controls Genes during the Switch from the Multipotent State to the Epidermal Fate. To characterize the role of p63 during epidermal commitment, we searched for genes that were potential direct targets of p63. We firstly identified

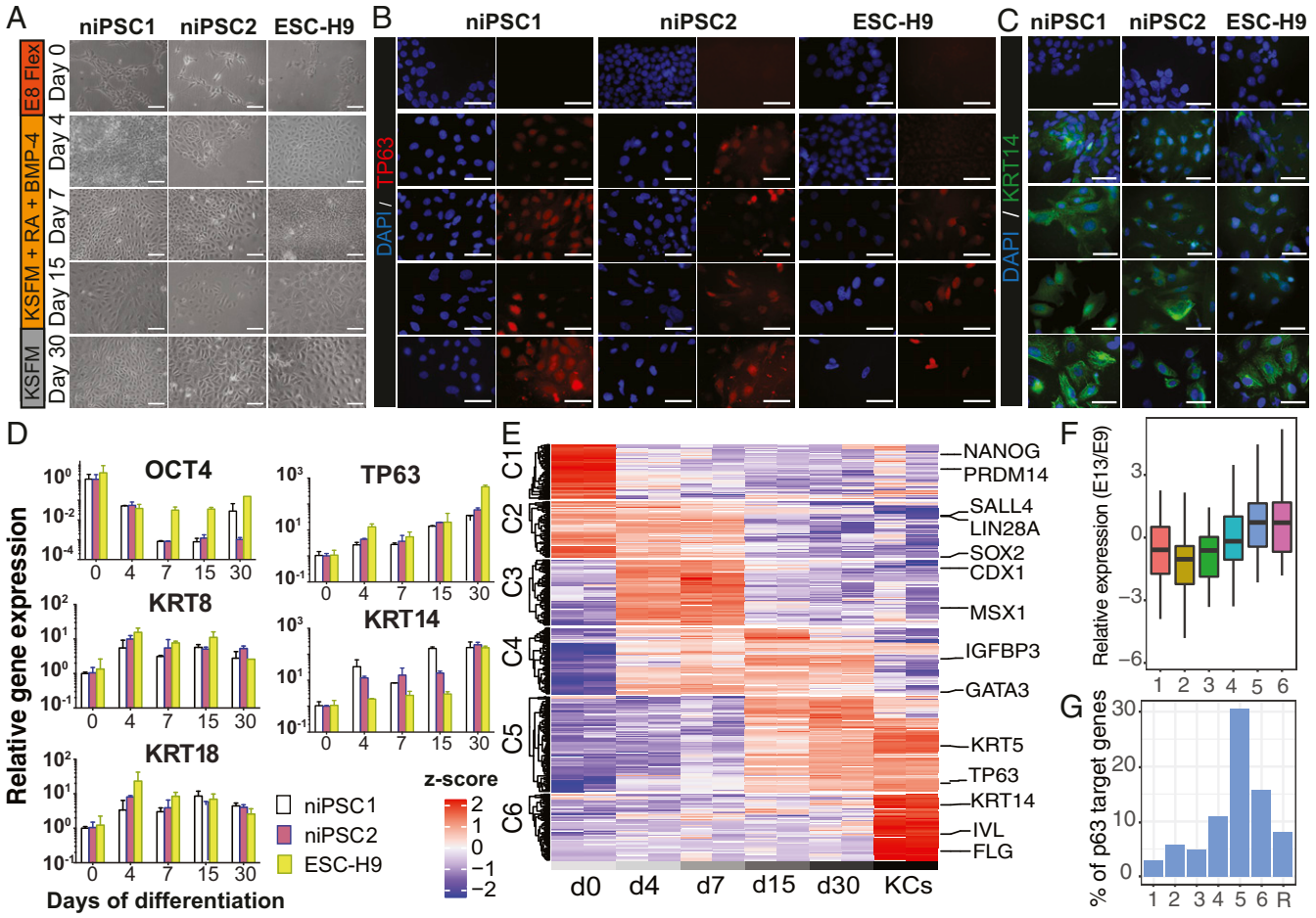

Fig. 1. Generation and characterization of iKCs using human PSCs. (*A*) The schematic protocol for PSCs differentiation toward iKCs is perpendicularly presented to the bright field images of 3 different control PSC cell lines (niPSC1, niPSCs2, and ESC-H9) that were induced for epidermal differentiation. (Scale bars, 100 μm.) (*B*) Immunofluorescence staining for p63 (red) on different days during differentiation (indicated in *A*). Cell nuclei were stained with DAPI (blue). (Scale bars, 50 μm.) (*C*) Immunofluorescence staining for *KRT14* (green) during differentiation. Cell nuclei were stained with DAPI (blue). (Scale bars, 50 μm.) (*D*) qRT-PCR analysis of marker genes during differentiation. Gene expression is expressed as ratio over *GUSB* and undifferentiated day-0 samples for each cell line ($n = 2$ per group). Data are presented as mean ± SD. (*E*) Heatmap of 6 clusters of DE genes in PSCs (niPSC1) during differentiation and in human primary KCs. The colors in the heatmap indicate high (red) or low (blue) expression across the sample set. (*F*) Relative gene expression presented in the log scale of ratios between the epidermis in E13 to E9 in mouse embryos. The genes included in this plot are differentially regulated genes in 6 clusters in *E*. (*G*) Percentage of potential p63 target genes in each of the 6 clusters in *E*. The potential p63 targets were mapped using dynamic p63 enhancers.

p63-bound enhancers that were dynamically changed during commitment. For this, we utilized p63 binding sites identified by p63 ChIP-seq in epidermal KCs (GEO: GSE119997) (22) and open chromatin regions identified by assay for transposase accessible chromatin followed by sequencing (ATAC-seq) generated during ESC epidermal commitment (GEO: GSE108248) (23). We took this approach because the p63 protein level was low at the initiation stage of iPSC epidermal commitment, and p63 ChIP-seq using differentiated iPSCs was likely unreliable. A total number of 9,361 genomic binding regions of p63 (p63 binding sites) were clustered to 4 groups using ATAC-seq intensity obtained during ESC epidermal commitment. Among them, only cluster 4 p63 binding sites (2,454 peaks in 9,361) were induced consistently during epidermal commitment and ATAC-seq signals remained at a high level in epidermal keratinocytes (*SI Appendix*, Fig. S2*G*). In parallel, we also examined p63 binding sites using an ATAC-seq analysis generated using p63 knockout ESC cells (23). Only 10% of these sites (cluster 3; 794/9,361) did not seem to fully lose ATAC-seq signals in p63 knockout cells (*SI Appendix*, Fig. S2*H*). These findings indicate that the large majority of p63 binding sites identified in KCs are indeed dependent on p63 expression. Subsequently, we overlapped induced p63 enhancers (cluster 4 in *SI Appendix*, Fig. S2*G*) and p63-dependent enhancers (clusters 1 and 2 in *SI Appendix*, Fig. S2*H*), and obtained 2,226 sites that were considered p63-dependent dynamic enhancers during epidermal commitment, thereafter termed "dynamic p63 enhancers."

We then used these 2,226 dynamic p63 enhancers to map potential p63 direct target genes in the 6 clusters of differentially regulated genes (Fig. 1*G*). Intriguingly, cluster 5 that contains genes induced on days 15 and 30 during epidermal commitment showed the highest percentage of potential direct p63 targets, significantly higher than the random expectation (P value = 2.2e-16) and that of any other clusters (Fig. 1*G* and *SI Appendix*, Fig. S2*F*), indicating that p63 controls the cell specification switch from multipotent state to the epidermal fate. Furthermore, cluster 1, 2, and 3 genes that were expressed at high levels at early differentiation stages (days 0 and 4) when p63 expression was barely detectable had even lower percentages than the random expectation (P value = 3.0e-13, 5.2e-05, and 2.0e-07, respectively), demonstrating that these genes are not under the control of p63. As comparison, we also mapped p63 binding sites to potential target genes, using ChIP-seq data obtained from ESCs on differentiation day 7 or from epidermal KCs (22, 23).

There was no significant enrichment or less significant enrichment of p63 targets in cluster 5 genes, respectively, as compared to the random expectation (*SI Appendix*, Fig. S2*F*). These findings showed that using these 2,226 dynamic p63 enhancers is a preferred method to identify direct p63 target genes during epidermal commitment.

Differentiation Defects of PSCs Carrying p63 EEC Mutations during Epidermal Commitment. Next, we examined the p63 function in epidermal specification by analyzing the effect of p63 EEC mutations during epidermal commitment. For this, we used 2 previously described iPSC lines derived from EEC patients who carry mutations in the p63 DNA-binding domain, R204W or R304W (18), termed EEC-iPSCs. The mutations in these iPSCs were confirmed by Sanger sequencing analyses (*SI Appendix*, Fig. S3*A*). The morphology of control PSCs and EEC-iPSCs at the undifferentiated and early differentiation stages (days 0 and 4) was indistinguishable (Figs. 1*A* and 2*A*). Morphological differences between control PSCs and mutant iPSCs became evident from differentiation day 7. Many EEC-iPSCs lost the typical cobblestone shape, started to detach from culture plates, and few cells survived until day 30 (Fig. 2*A*). qRT-PCR analyses showed that *OCT4* expression decreased, and simple epithelial gene *KRT8* and *KRT18* expression was not significantly different in all PSCs (Fig. 2*B*). This is expected, as these gene are known not to be under the control of p63 (14). In contrast, the epidermal markers p63 and KRT14 whose expression was progressively increased in control PSCs (Fig. 1 *B*–*D*) was significantly affected in EEC-iPSCs (Fig. 2 *B* and *C* and *SI Appendix*, Fig. S3*C*).

To corroborate that impaired commitment indeed results from p63 EEC mutations, we generated PSCs that contained the EEC R304W mutation on isogenic backgrounds of control PSCs. This was performed by introducing the mouse p63 R304W mutant into control iPSC1 (niPSC1) and ESC-H9, termed iso-R304W PSCs. Expression of the MYC-tagged p63 R304W mutant transgene was confirmed by immunostaining (Fig. 2*D*) and by sequencing of the cDNA derived from iso-R304W PSCs (*SI Appendix*, Fig. S3*B*). During differentiation of these iso-R304W PSCs, heterogeneous cell morphology was observed (*SI Appendix*, Fig. S3*D*), similar to the morphology detected during EEC-iPSC differentiation (Fig. 2*A*). Importantly, in contrast to the strong induction of epidermal marker *KRT14* in the isogenic niPSC1 on differentiation day 15, no induction was observed in both iso-R304W PSCs (Fig. 2 *D* and *F*). qRT-PCR analyses also showed consistent marker gene expression, as compared to EEC-iPSCs (*SI Appendix*, Fig. S3*E*). The expression of *TP63* in iso-R304W PSCs stayed unchanged (*SI Appendix*, Fig. S3*E*), as the mouse p63 R304W mutant was expressed constitutively in these cells. These data unambiguously demonstrated that the expression of the mutant p63 in PSCs abrogate the function of the normal p63 and affects the switch from the multipotent simple epithelial state to the epidermal fate during epidermal commitment. These findings also consolidate the dominant negative model of p63 EEC mutations proposed previously (7).

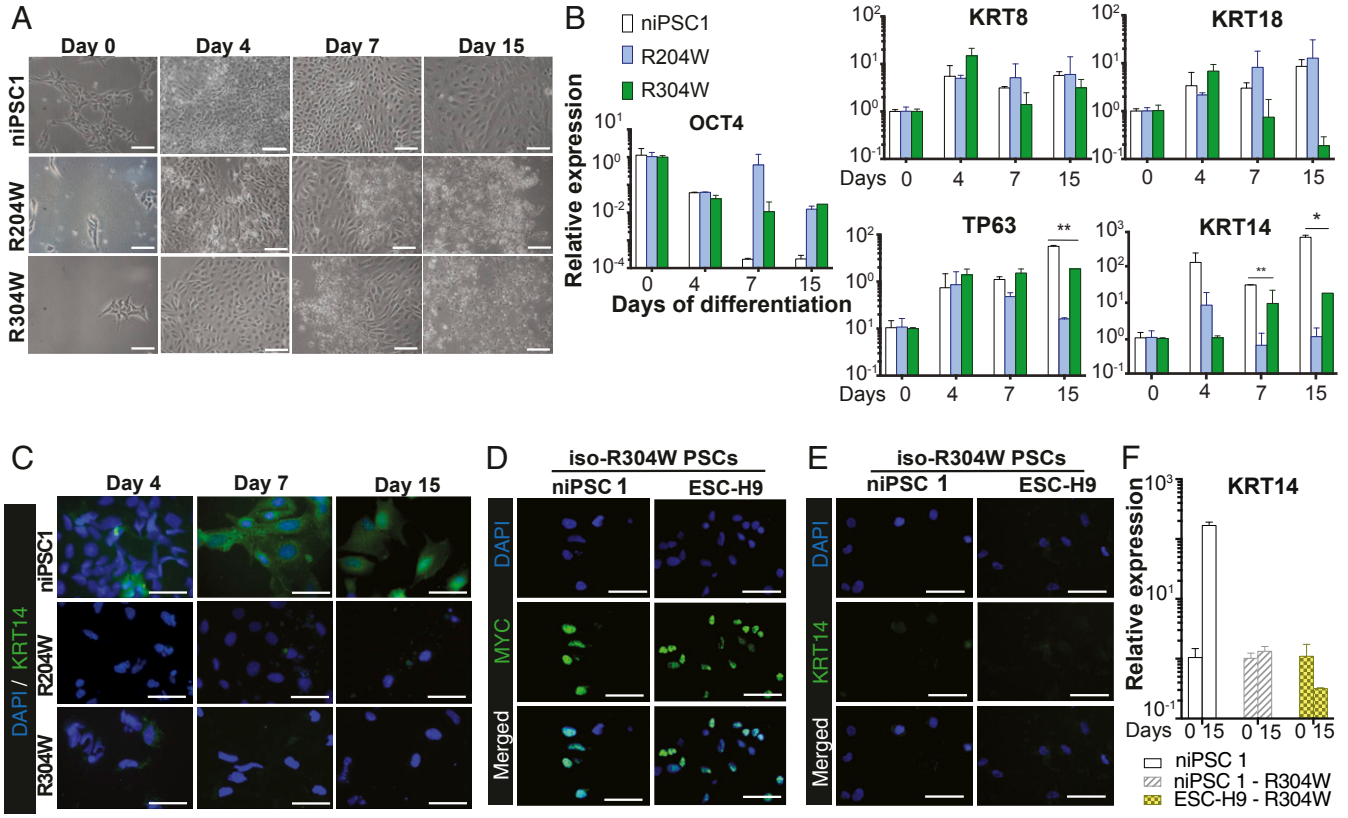

Fig. 2. Differentiation defects of PSCs carrying p63 EEC mutations. (*A*) Bright field image of patient-derived EEC-iPSCs, R204W and R304W, during epidermal differentiation until day 15. (*B*) qRT-PCR analysis of marker gene expression in control niPSC1 and EEC-iPSCs. Gene expression is expressed as the ratio over *GUSB* and undifferentiated day-0 samples for each cell line ($n = 2$ per group). Data are presented as mean ± SD, $*P < 0.05$, $**P < 0.01$. (*C*) Immunofluorescence staining for KRT14 (green) and DAPI (blue) in niPSC1 and EEC-iPSCs during differentiation. (Scale bars, 50 μm.) (*D*) Immunofluorescence staining for the MYC-tag (green) and DAPI (blue) in iso-R304W PSCs (niPSC1-R304W and ESC-H9-R304W) on day 15. (Scale bars, 50 μm.) (*E*) Immunofluorescence staining for the epidermal marker KRT14 (green) and DAPI (blue) in iso-R304W PSCs (niPSC1-R304W and ESC-H9-R304W) on day 15. (Scale bars, 50 μm.) (*F*) qRT-PCR analysis of the epidermal marker *KRT14* expression in control niPSC1 and iso-R304W PSCs. Gene expression is expressed as the ratio over *GUSB* and undifferentiated day-0 samples for each cell line ($n = 2$ per group). Student's *t* test was performed comparing the committed cells against day 0, for each genotype. Data are presented as mean ± SD.

Deregulated Epithelial Gene Expression in Differentiating PSCs Carrying p63 EEC Mutations. To characterize EEC-iPSC commitment at the molecular level, we performed RNA-seq analysis of these cells during epidermal differentiation (*SI Appendix*, Fig. S4*B* and Dataset S1). K-means clustering analysis of the top 500 DE genes identified 7 clusters (Fig. 3*A*, *SI Appendix*, Fig. S4*A*, and Dataset S4). Generally, the expression pattern of these 7 clusters of genes was consistent with that in control PSCs during differentiation, with down-regulated genes in clusters 1 and 2 playing roles in stem cell maintenance and genes in clusters 3 and 4 that were initially induced and subsequently down-regulated functioning in morphogenesis. Cluster 6 included genes that were up-regulated during differentiation, and many are known for a role in epidermal development. For some of these genes, there was no obvious difference between control PSCs and EEC-iPSCs.

Among the 7 clusters, 2 clusters, clusters 5 and 7, showed a clear difference between control PSCs and EEC-iPSCs at later stages of differentiation (day 7 onwards) when p63 expression became readily detectable (Fig. 3*A* and *SI Appendix*, Fig. S4*A*). Cluster 5 contained genes that were expressed at a higher level in EEC-iPSCs at differentiation stages on days 7 and 15, as compared to control PSCs. These genes were strongly enriched for functions in immune and defense response, such as *IFNB1* and *IFIT1*. Cluster 7 genes were strongly up-regulated in control PSCs at late differentiation stages on day 15 and day 30, but remained consistently low in EEC-iPSCs. Genes in this cluster included *KRT5* and *KRT1* that have important roles in regulating epidermal development. This deregulated gene expression pattern, accompanied by differentiation defects of EEC-iPSCs observed at this stage, showed that these 2 clusters of genes are deregulated due to p63 EEC mutations.

To corroborate these observations from in vitro human iPSC differentiation with in vivo development controlled by p63, we compared expression of cluster 5 and 7 genes with expression of genes that were deregulated in the embryonic epidermis of a p63 knockout model (21). Cluster 5 genes that contains many nonepithelial genes (e.g., immune genes) and were expressed at high levels in EEC-iPSCs had high expression in the p63 KO epidermis. In contrast, cluster 7 genes that includes many epidermal genes and were down-regulated in EEC-iPSCs had high expression levels in the mouse embryonic epidermis where p63 function is normal (HET) (Fig. 3*B*). Furthermore, we examined whether these cluster 5 and 7 genes were p63 direct targets by using the 2,226 dynamic p63 enhancers. Cluster 7 genes were highly enriched for p63 direct targets, as compared to the random expectation (P value = 2.2e-16), whereas cluster 5 genes that mainly play roles in nonepithelial functions did not have enriched p63 targets and were likely not p63 direct targets (Fig. 3*C*). These findings show that gene expression dynamics observed during iPSC differentiation is consistent with in vivo epidermal development and suggest that p63 directly controls epidermal gene activation during commitment. Nonepithelial gene activation is probably an indirect effect caused by p63 EEC mutations.

To further assess the gene expression difference between control PSCs and EEC-iPSCs, we looked for consistent DE genes that were common to both EEC mutations, R204W and R304W, on differentiation day 15 (*SI Appendix*, Fig. S4*C* and Dataset S5). Commonly down-regulated genes (241) in EEC-iPSCs were related to epithelial and epidermal development (e.g., *KRT5* and *S100A9*), whereas up-regulated genes (296) in both EEC-iPSCs were enriched in functions such as cell migration (*IGFBP5*) and nonepithelial functions such as immune response (*IFIT2*) (*SI Appendix*, Fig. S4*D* and Dataset S5). We subsequently chose several deregulated typical epidermal and nonepidermal genes and validated their expression in control PSCs, EEC-iPSCs, and the isogenic iso-R304W PSCs by qRT-PCR analyses. Our analyses confirmed that epidermal genes *KRT14*, *COLA17A1*, and *ITGB4* were consistently down-regulated in EEC-iPSCs and in isogenic iso-R304W PSCs, whereas nonepithelial genes *VIM* and *MSX1* were up-regulated, as compared to control PSCs (Fig. 3*D*). The up-regulation of *VIM* in EEC-iPSCs was also confirmed at the protein level (Fig. 3*E*). These

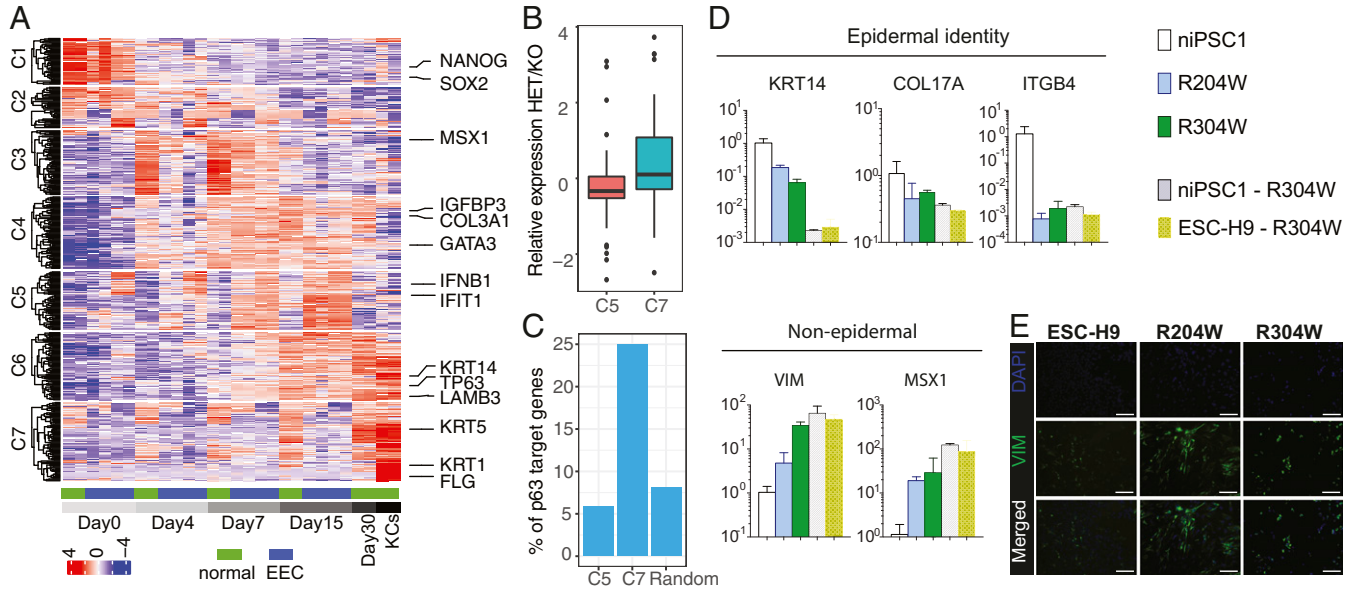

Fig. 3. Deregulated epithelial gene expression in PSCs carrying p63 EEC mutations. (*A*) Heatmap of 8 clusters of DE genes in PSCs (niPSC1) and EEC-iPSCs during differentiation and in KCs. The colors in the heatmap indicate high (red) or low (blue) expression across the sample set. (*B*) Relative gene expression presented in the log scale of ratios between normal (HET) to KO mouse embryonic epidermis. The genes included in this plot are those in clusters 5 and 7 in *A*. (*C*) Percentage of potential p63 target genes in clusters 5 and 7 in *A*. The potential p63 targets were mapped using dynamic p63 enhancers. (*D*) qRT-PCR analysis of epithelial *KRT14*, *COL17A1*, and *ITGB4* and known nonepidermal genes *VIM* and *MSX1* in control niPSC1, EEC-iPSCs, and isoR304W-PSCs on differentiating day 15. Gene expression is expressed as the ratio over *GUSB* and niPSC1 for each gene (n = 2 per group). (*E*) Immunfluorescence of VIM in control ESC-H9 and EEC-iPSCs on day 15. (Scale bars, 100 μm.)

data agree with the previous study showing differentiation defects of EEC-iPSCs and up-regulation of mesodermal genes during epithelial commitment (14), suggesting that the acquisition of the epithelial fate is impaired in EEC-iPSCs.

Cell State Heterogeneity during Differentiation Identified by Single-Cell RNA-Seq. As differentiating PSCs are heterogeneous, to identify cell states associated with EEC-iPSCs that failed to commit to the epithelial fate, we performed single-cell RNA-seq using a modified single-cell tagged reverse-transcription sequencing (STRT-seq) protocol (24). In total, we analyzed the transcriptome of 1,250 single cells from control PSCs and EEC-iPSCs at different differentiation stages, as well as from primary KCs of a control and of the same EEC patients carrying R204W and R304W. After filtering based on the data quality (*SI Appendix*, Fig. S5), we obtained the transcriptome of 964 single cells. Following normalizations to get rid of batch effects (25), we detected 500 DE genes and performed PCA analysis (Fig. 4*A*). Upon differentiation, DE gene expression of all PSCs showed a triangle-shape transition in PCA. Genes associated with PC1 (14.5%) showed an enrichment for functions in epidermal and epithelial development, whereas genes associated with PC2 (11.4%) were more enriched for migration, defense, and extracellular matrix functions (Fig. 4*B* and Dataset S6). On day 15, DE genes reached the highest level along PC2, with those of EEC-iPSCs higher than those of control PSCs. DE genes of day-30 iKCs moved down along PC2 toward primary KCs. The PCA analysis suggests that control PSCs went through an intermediated phase before committing to iKCs, and EEC-iPSCs did not switch to the route toward the epidermal fate. Furthermore, t-distributed stochastic neighbor embedding (t-SNE) analysis showed that control PSCs and EEC-iPSCs before differentiation clustered together, and upon differentiation induction when p63 expression became detectable, differentiating control PSCs and EEC-iPSCs clustered into distinct groups (*SI Appendix*, Fig. S6*B*). These findings are consistent with differentiation defects observed in differentiating EEC-iPSCs and with the data from the bulk RNA-seq analyses, suggesting that expression of mutant p63 gave rise to distinct cell states.

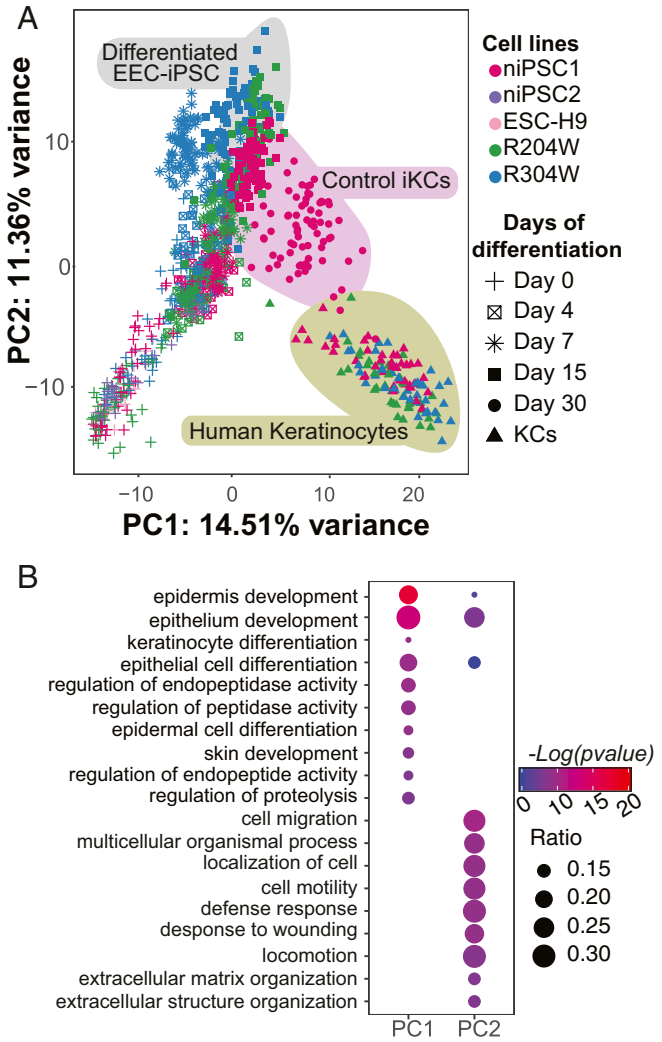

Fig. 4. Cell state heterogeneity during differentiation identified by single-cell RNA-seq. (*A*) PCA of the top 500 highly variable (HV) genes obtained from single-cell RNA-seq during epidermal differentiation of PSCs and primary KCs. Colors represent cell lines; shapes represent differentiation days. (*B*) GO analysis showing biological process terms enriched for PC1 and PC2 axes. The gene ratio is indicated by the dot sizes and the significance by the color of the dot (red, low *P* value; blue, high *P* value).

For identifying cell fates, we deconvoluted bulk RNA-seq data of cells derived from different embryonic origins (the ENCODE data and GEO: GSE101661) (26) using our single-cell transcriptome. As expected, the starting PSCs showed high correlations with ESC-H9 bulk RNA-seq data, and the correlations decreased when PSCs were induced for differentiation (*SI Appendix*, Fig. S6*C*). In addition, primary control KCs, EEC-KCs, and day-30 control iKCs showed high correlations with the 2 types of epithelial cells, normal human epidermal keratinocytes (NHEKs) and human mammary epithelial cells (HMECs) (*SI Appendix*, Fig. S6*C*). These high correlations were also consistent with the high expression level of *KRT5* in these cell types (*SI Appendix*, Fig. S7 *A* and *B*). Furthermore, it is noticeable that differentiating control PSCs on day 15 showed the highest correlation with embryonic cells (*SI Appendix*, Fig. S6*C*). These data indicate that a multipotent cell state is established at early stages during normal PSC differentiation, before the switch toward epidermal fate. When interrogating the cell state of differentiating EEC-iPSCs on day 15, the most striking observation was the high correlation of EEC-iPSCs with nonepithelial cells, human skeletal muscle myoblasts (HSMMs), normal human lung fibroblasts (NHLFs), human umbilical vein endothelial cells (HUVECs), and ESC-derived other cell types (*SI Appendix*, Fig. S6*C*). The correlations were consistent with higher expression of nonepithelial genes such as *VIM*, *MMP*, and *IFIT* genes in EEC-iPSCs, especially in R304W-iPSCs (*SI Appendix*, Fig. S7 *A* and *B*). These findings indicate that EEC-iPSCs exhibited an enhanced nonepithelial cell state, arguing that they retained the multipotent cell state and that differentiation defects caused by p63 EEC mutations occurred during the switch to the epidermal fate.

In summary, the single-cell transcriptome data demonstrated the cell state heterogeneity during in vitro PSC epidermal commitment. Collectively, our temporal transcriptome analyses indicate that the normal epidermal commitment process consists of several connected yet distinct phases. Furthermore, differentiated PSCs carrying EEC p63 mutations retained nonepithelial cell identity, suggesting that these mutations disturbed the switch from the multipotent state to the basal stratified epithelial fate, and p63 expression is not sufficient for epidermal maturation.

Deviated Commitment Route with Enhanced Nonepithelial Cell Fates in EEC-iPSC Differentiation. To identify the timing of affected cell states and the potential alternative differentiation route of EEC-iPSCs, we examined differentiation trajectories of PSCs toward KCs using pseudotime analysis Monocle (15). When cells were ordered according to gene expression pseudotime, control PSCs exhibited a switch at day 7 and day 15, and then progressed on the path toward primary KCs, even though most day-30 control

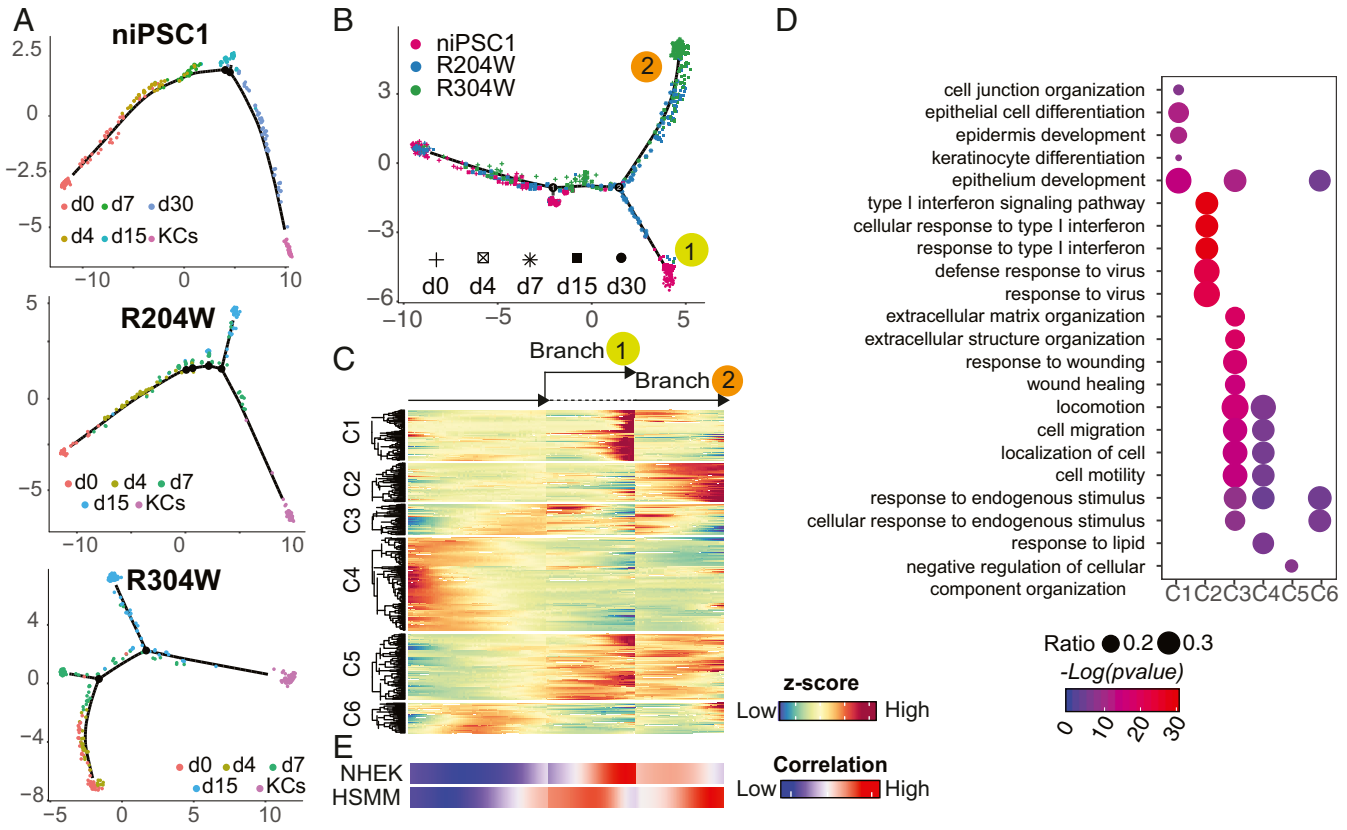

Fig. 5. Deviated commitment route with enhanced nonepithelial cell fates in EEC-iPSC differentiation. (*A*) Differentiation gene expression trajectories of control niPSC1 and EEC-iPSCs during differentiation and that of primary KCs using pseudotime (Monocle) analysis. Differentiation days are indicated by colors. (*B*) Differentiation gene expression trajectories of control niPSC1 (pink) and EEC-iPSCs, R204W-iPSCs (blue), and R304-iPSCs (green) during differentiation using pseudotime (Monocle) analysis, without primary KCs. Differentiation days are indicated by shapes. (*C*) Heatmap of 6 clusters of DE genes detected by pseudotime analysis based on their Z-scores (indicated by the color). (*D*) GO analysis showing biological process terms enriched for DE genes in each cluster. The gene ratio is indicated by the dot size and the significance by the color of the dot (red, low *P* value; blue, high *P* value). (*E*) Correlation of the single-cell transcriptome against bulk RNA-seq data of NHEKs and HSMMs. Correlation coefficient is indicated by color.

PSCs did not reach the primary KC state (Fig. 5*A*). In contrast, differentiated EEC-iPSCs were more heterogeneous and diverted toward other directions. Although both EEC-iPSC lines had a small number of cells moving in the pseudotime path toward primary KCs, R304W-iPSCs showed more subbranches and more cells at subbranches than that of R204W-iPSCs, suggesting more severe differentiation defects (Fig. 5*A*). When primary KC profiles were excluded in the analysis, the bifurcation that occurred on day 7 and day 15 between control PSCs and EEC-iPSCs became more apparent (Fig. 5*B*). The pseudotime path of differentiated R304W-iPSCs and the majority of R204W-iPSCs took an alternative direction (branch 2 in Fig. 5*B*) other than the path of control PSCs. According to the pseudotime ordering, differentially regulated genes were clustered into 6 clusters, and cluster 1 and 2 genes corresponded to the bifurcation branches 1 and 2, respectively (Fig. 5*C*). GO analyses of cluster 1 genes showed that these genes were associated with epidermal development and keratinocyte differentiation, whereas that of cluster 2 genes showed an enrichment of genes involved in immune response (Fig. 5*D* and Dataset S7). In agreement, correlation analyses to bulk RNA-seq data showed that genes enriched for branch 1 cells had a higher correlation to gene signatures of epithelial NHEK and HMEC cells, and genes enriched for branch 2 cells correlated better to HSMM and other nonepithelial cells (Fig. 5*E* and *SI Appendix*, Fig. S6*C*). Genes in other clusters were expressed earlier during differentiation (Fig. 5 *B* and *C*). These data demonstrated that the differentiation route of EEC-iPSCs largely deviated from the normal commitment route toward the epithelial fate. The deviation occurred at the multipotent state on differentiation days 7 and 15 when p63 expression was detectable, prior to epidermal maturation.

Epidermal Differentiation Enhanced by Inhibitors of Mesodermal Induction. As differentiated EEC-iPSCs had higher expression of immune response genes and a higher correlation with HSMM, we reasoned that these differentiated EEC-iPSCs exhibited an enhanced mesodermal identity, as both the immune system and skeletal muscles derive from the mesoderm. To directly assess whether the mesodermal activation is associated with the commitment defects of EEC-iPSCs and whether repressing mesodermal activation can enhance epidermal differentiation of EEC-iPSCs, we tested 3 inhibitors that can repress mesodermal induction, heparin, valproic acid (VA), and suramin (27–29). Given that PSCs entered a multipotent state on differentiation day 7, and p63 started to be highly expressed and exerted its role to activate epidermal genes for epidermal commitment (Fig. 1 *B*, *E*, and *G*), we decided to include these inhibitors in the differentiation medium from day 7 onwards (Fig. 6*A*). For these experiments, we chose to use the R304W mutant, as R304W-iPSCs gave the most severe defects during differentiation and additional iso-R304W PSC lines were available to be tested in parallel. Without treatment, differentiating R304W-iPSCs and iso-R304W PSCs suffered from severe cell death in the normal differentiation medium on day 15 (Figs. 2*A* and 6*B*). Upon treatment, cells survived beyond day 15, especially in the suramin-containing

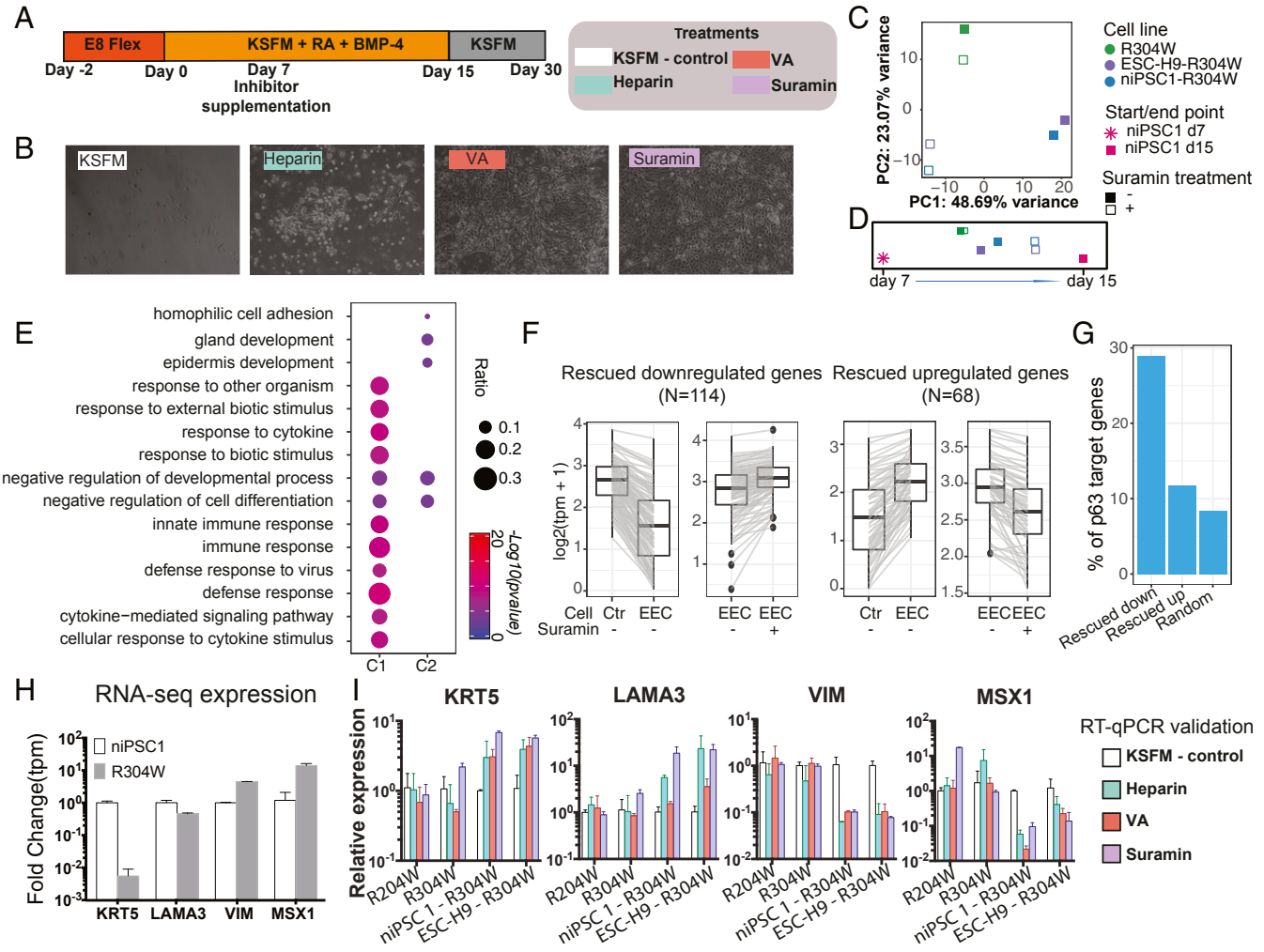

Fig. 6. Epidermal differentiation enhanced by compounds repressing mesodermal fate. (*A*) Scheme of supplementation of inhibitors, heparin, VA, or suramin, during epidermal differentiation. (*B*) Bright field images of R304W-iPSCs without Keratinocyte serum-free medium (KSFM) and with inhibitor treatment (heparin, VA, suramin) on day 15. (*C*) PCA plot of RNA-seq analyses of R304W-PSCs without (filled) and with (open) suramin treatment. (*D*) Gene expression of R304W-PSCs without (filled) and with (open) suramin treatment mapped onto the PCA plot generated initially with all control and EEC-i PSCs (*SI Appendix*, Fig. S4*B*), using gene expression of control iPSCs on days 7 and 15 as the start and end coordinates. (*E*) GO annotation of top genes associated with PC1 and PC2. (*F*) Expression of genes either down-regulated or up-regulated in EEC-i PSCs on differentiation day 15 and their expression with suramin treatment. (*G*) Percentage of potential p63 target genes among rescued genes. The potential p63 targets were mapped using dynamic p63 enhancers. (*H*) Fold change difference of gene expression between niPSC1 and R304W on day 15, detected by bulk RNA-seq. (*I*) qRT-PCR analysis of rescued genes in R204W and R304W-PSCs treated with inhibitors on day 15. Gene expression is expressed as the ratio over *GUSB* and day-15 PSCs without treatment ($n = 2$ per group).

medium, and differentiated PSCs had a cobblestone morphology that was similar to primary KCs on day 15 (Fig. 6*B*).

To identify the global gene expression change and pathways associated with suramin treatment, RNA-seq analyses were performed. PCA analysis (Fig. 6*C* and Dataset S8) showed significant changes in the transcriptome for iso-R304W PSCs (both PC1 and PC2) and less significant changes for R304W-iPSCs (PC2). GO analysis of genes associated with PC1 showed enrichment of genes associated with immune and defense response, whereas genes associated with PC2 that were rescued in all R304W cells were enriched for genes important for epidermal development, such as *KRT5* and *EDAR2* (Fig. 6*E* and *SI Appendix*, Fig. S8). To better examine whether suramin-treated R304W PSCs were indeed more similar to controls cells, we mapped the transcriptome of suramin-treated PSCs into the differentiation trajectory of niPSC1 between differentiation days 7 and 15 (Fig. 6*D*), using initial PCA of all PSCs (*SI Appendix*, Fig. S4*B*). This analysis showed that, at the global level, the gene expression of untreated EEC PSCs including EEC-iPSCs and iso-R304W PSCs was between niPSC1 on day 7 and day 15, consistent with our previous bulk RNA-seq experiment (*SI Appendix*, Fig. S4*B*). The suramin treatment indeed pushed EEC PSCs closer to niPSC1 on day 15, with more significant effect on iso-R304W PSCs. Among 241 down-regulated genes in both EEC-iPSCs on differentiation day 15 (*SI Appendix*, Fig. S4*C*), 114 genes were rescued by suramin (Fig. 6*F*). Many of these genes play roles in epidermal development (e.g., *KRT5*) and in adhesion and extracellular matrix (e.g., *DSG3*) (Dataset S8). Among 296 up-regulated genes in EEC-iPSCs (*SI Appendix*, Fig. S3*F*), only 68 genes were rescued (Fig. 6*F*), and many are known in neural and vascular endothelial function (Dataset S8). Furthermore, potential p63 direct targets mapped by dynamic p63 enhancers were highly enriched among rescued 114 genes that were down-regulated in EEC-iPSCs (P value = 2.2e-16), but not among 68 genes that were up-regulated in EEC-iPSCs (Fig. 6*G*). We subsequently validated several typical epidermal and mesodermal genes by qRT-PCR analysis. Indeed, epidermal genes that are down-regulated in R304W iPSCs such as *KRT5*

and *LAMA3* were rescued by suramin treatment, as well as up-regulated mesodermal genes in R304W iPSCs such as *VIM* and *MSX1* (Fig. 6*I*), consistent with our RNA-seq analyses (Fig. 6*H* and *SI Appendix*, Fig. S8). Some of these genes were also partially rescued by heparin and VA, but to a lesser extent (Fig. 6*I*).

Discussion

The role of p63 in controlling the integrity of stratified epithelial tissues, especially how p63 mutations associated with developmental disorders affect these tissues, remains largely unexplored. In this study, we characterized molecular signatures of cell fate transitions using epidermal commitment as the model, and dissected how this process is affected in EEC syndrome. Using bulk and single-cell transcriptome analyses, we showed that PSCs commitment toward the epidermal fate includes several connected yet distinguishable phases: 1) PSC commitment toward the multipotent simple epithelial fate; 2) the switch from the simple epithelium to the basal stratified epithelial fate; and 3) maturation of the epidermal fate. Single-cell analyses identified the timing and the alternative route of differentiation defects associated with p63 EEC mutations that occurred during the switch from the multipotent to the epidermal fate, prior to epidermal maturation. As the differentiation route of EEC PSCs exhibited enhanced mesodermal signatures, we tested inhibitors that repress mesodermal induction and showed that these inhibitors could enhance epidermal commitment.

Stratified epithelia are multilayered structures found in many organs as the outer surface such as the epidermis or lining of internal organs such as the bladder. Although they may be different from their biological functions and from their embryonic origins, stratified epithelia share similarities in their transcriptional programs (4, 5). For example, high expression of *KRT5* and *KRT14* is found in the basal cells of these epithelia. In our experiments, although PSCs started to change morphology to a cobblestone shape that was similar to primary KCs already on differentiation day 4, the molecular signature represented a simple epithelial signature. The day-30 iKCs showed several molecular hallmarks of epidermal cells, with up-regulated *KRT5* and *KRT14* and down-regulate *KRT8* and *KRT18* (Fig. 1 *A*–*D*), and could even be further induced toward terminal stratification (*SI Appendix*, Fig. S2 *A* and *B*). However, our transcriptome analyses showed that the day-30 iKCs did not have the same molecular signature as the primary KCs, thus not the same cell state (Fig. 1*E*). This indicates that day-30 iKCs may retain some embryonic properties. Retaining embryonic signatures seems to be a common phenomenon for iPSC-derived cell types (30). Alternatively, they may represent a mixture of basal epithelial cells that can stratify, as *KRT8* and *KRT18* are expressed in some stratified epithelial cells such as those in mammary glands (31). Therefore, simply relying on cell and tissue morphology and expression of a limited number of marker genes to study cell commitment is probably not sufficient for distinguishing similar yet distinct cell states. In our pseudotime analysis of the single-cell RNA-seq data, we observed heterogeneous cell populations in differentiated EEC-iPSCs. Although the majority of cells deviated from the route toward epidermal cells, showing the importance of p63 controlling the epidermal commitment, a small percentage of R204W and R304W iPSCs were still on the path toward the epidermal fate, even though their cell states were distinct from the mature epidermal fate (Fig. 5*A*). This intriguing observation is reminiscent of the heated debate on the role of p63 either in epidermal commitment or in stem cell maintenance, partially due to using different mouse models (2–5, 12–14). Our findings highlight the importance of using comprehensive (single cell) transcriptome analysis to identify molecular signatures and proper cell states. This approach may assist in scrutinizing the p63 function in epidermal development where different roles may not be mutually exclusive.

Our study dissected the epidermal commitment and maturation process in detail, showing that connected yet distinct phases are involved in the process. Proper p63 expression and function are required for the switch from the multipotent state to the epidermal fate, and p63 EEC mutations disturbed this switch. The detrimental function of p63 during the switch, probably before the maturation of epidermal cells, is consistent with defects in all stratified epithelia observed in p63-deficient mouse models (2, 3) and in human diseases associated with p63 mutations (6). In line with previous observations of up-regulated mesodermal gene expression in p63-deficient models (14), we showed that the mesodermal cell identity was enhanced in PSCs carrying p63 EEC mutations. However, rather than simply being blocked between the ectodermal and fully committed epidermal stage, suggested by p63-deficient mouse studies (14), our single-cell transcriptome and pseudotime analyses showed that the majority of differentiated EEC PSCs deviated from the normal route of epidermal commitment to a more mesodermal cell identity (Fig. 5). Between the 2 EEC mutants, R304W mutation seemed to more severely affect the normal differentiation route than R204W, which is consistent with the reported difference of these 2 mutants (18, 32). A role of p63 in repressing epithelial mesenchymal transition (EMT) has previously been reported for epithelial-related cancers, such as squamous cell carcinoma and breast cancer (33). The observed mesodermal activation in EEC PSCs resembles EMT in cancers and may represent an embryonic EMT that is repressed by p63 during development. This interpretation is consistent with a recent report on p63 using mouse embryonic epidermis (21). To address the question whether p63 represses mesodermal genes directly or the repression is an indirect effect, we showed that the percentage of p63 direct targets among these mesodermal genes was significantly lower than epithelial and epidermal genes that are normally activated by p63, and even lower than the random expectation (Fig. 3*C*). This indicates that the predominant role of p63 is to activate epithelial and epidermal genes, and repressing mesodermal induction is probably indirect. However, a small number of mesodermal genes activated in EEC PSCs (cluster 5) or in mouse p63 KO cells did contain a dynamic p63 binding site nearby (Fig. 3*C* and Dataset S5), suggesting that they might be p63 direct targets. The observed mesodermal activation could also be partially due to expansion of nonepithelial cells in the heterogeneous differentiated iPSC population.

All 3 inhibitors of mesodermal induction tested in this study, heparin, VA and suramin, are known to repress the mesodermal lineage or interfere with EMT (27, 29). Suramin seemed to be more efficient in rescuing differentiation defects of EEC PSCs than heparin and VA. These differences may result from different working mechanisms of these compounds. Heparin can bind to fibroblast growth factors (FGFs) and modulate their signaling pathways (34). VA is a histone deacetylase inhibitor that can up-regulate H3 acetylation and repress EMT (28). Although sumarin is well known for its antiviral and antiparasite effects (35), it was shown to inhibit mesodermal induction and formation in early *Xenopus* and sea urchin embryos (29, 36). It is a potent inhibitor for several growth factors, including the vascular endothelial growth factor (VEGF) (37) and FGFs (38) to inhibit angiogenesis. In addition, suramin has also been shown to enhance epithelial cell proliferation, probably through epithelial growth factor (EGF)-related pathways (39). It is plausible that sensitization of EGF signaling by suramin in epithelial cells contributes to the improvement of epidermal commitment of EEC-PSCs, as several genes involved EGF signaling such as STAT5A and PTGE (40, 41) as well as many epithelial genes such as S100A9 and GJB5 were up-regulated with suramin treatment (*SI Appendix*, Fig. S8). It seems unlikely that repression of mesodermal activation is through a p63-dependent pathway, as the number of p63 potential target genes in this category is low, similar to random expectation (Fig. 6*G*). In contrast, the suramin-induced epithelial and epidermal genes have a significantly higher number of p63 target genes (Fig. 6*G*). However, whether activation of these genes is via reactivating mutant p63, similar to other previously reported small molecule compounds (18, 32) or through an independent route would be of importance to further investigate.

Nevertheless, our rationalized compound testing provides promising future directions for therapeutic development of diseases associated with p63 mutations, not only for the epidermal phenotype but also for other stratified epithelia.

It should be noted that differentiation defects observed in our in vitro human PSC epidermal differentiation model was more severe than in EEC patient skin, as the skin phenotype of EEC patients is rather mild (6). This is probably due to the in vivo heterogeneous cell and tissue environment where other signals and pathways may compensate, e.g., those from the dermis that are probably independent on p63 (42). Nevertheless, our simplified in vitro differentiation assay sheds lights on the direct function of p63 and its regulatory gene network that is relevant to cell states and function. In summary, our study provides insights into the master regulatory function of p63 in early epidermal commitment and mechanisms underlying defects of stratified epithelia in disorders associated with p63 mutations. It also underscores the importance of single-cell transcriptomics in understanding the complex gene regulation in development and disease.

Materials and Methods

Detailed descriptions of methods and materials are presented in *SI Appendix*.

Control iPSCs Generation. Dermal fibroblasts of 2 health control individuals were reprogrammed into iPSCs by lentiviral transduction using the hOKSMcoidTomFRT plasmid (43). iPSCs carrying *TP63* mutations were described and characterized previously (18).

Differentiation of Human PSCs into iKCs. PSCs were seeded as single cells and induced with the keratinocyte induction medium with 10 ng/mL bone morphogenetic protein 4 (BMP4) (PromoKine) + 0.3 μg/mL RA (Sigma-Aldrich) (20). Inhibitors of mesodermal induction were included from day 7 in the induction medium.

Bulk RNA Sequencing Library Preparation and Analysis. The NuGEN Ovation RNA-seq (version 2, NuGEN) protocol was carried out for library preparation. All sample libraries were sequenced on Illumina HiSEq. 2500 (Illumina, San Diego). RNA sequencing data were processed by standard methods for mapping, differential gene expression, and GO term analyses.

Single-Cell RNA Sample Preparation. A modified STRT-seq protocol (24) was for the generation of single-cell transcriptome profiles. The main steps and the analysis pipeline are described in *SI Appendix*.

ACKNOWLEDGMENTS. We thank Ellen van den Bogaard and Matthijs Gerritse for discussion and for providing technical support, Ewart Kuijk and Edwin Cuppen for providing the ESC H9 line, and Eva Janssen-Megens, Siebe van Genesen, and Rita Bylsma for operating the Illumina analyzer and initial data output. We thank the Studer Lab (Sloan Kettering Institute, New York) and the ENCODE Consortium for sharing their data. This research was supported by Royal Dutch Academy of Science (KNAW/CEP 530-5CDP08), Netherlands Organisation for Scientific Research (NWO/ALW/MEERVOUD/836.12.010, H.Z.); a Radboud University fellowship (H.Z.); Brazilian Science without Borders program (E.S.); and Chinese Scholarship Council grants 201606230213 (Q.X.) and 201406330059 (J.Q.).

1. E. Soares, H. Zhou, Master regulatory role of p63 in epidermal development and disease. *Cell. Mol. Life Sci.* **75**, 1179–1190 (2018).
2. A. Yang *et al*., p63 is essential for regenerative proliferation in limb, craniofacial and epithelial development. *Nature* **398**, 714–718 (1999).
3. A. A. Mills *et al*., p63 is a p53 homologue required for limb and epidermal morphogenesis. *Nature* **398**, 708–713 (1999).
4. J. C. Pignon *et al*., p63-expressing cells are the stem cells of developing prostate, bladder, and colorectal epithelia. *Proc. Natl. Acad. Sci. U.S.A.* **110**, 8105–8110 (2013).
5. M. Senoo, F. Pinto, C. P. Crum, F. McKeon, p63 is essential for the proliferative potential of stem cells in stratified epithelia. *Cell* **129**, 523–536 (2007).
6. T. Rinne, H. G. Brunner, H. van Bokhoven, p63-associated disorders. *Cell Cycle* **6**, 262–268 (2007).
7. J. Celli *et al*., Heterozygous germline mutations in the p53 homolog p63 are the cause of EEC syndrome. *Cell* **99**, 143–153 (1999).
8. H. G. Brunner, B. C. Hamel, H. Van Bokhoven, The p63 gene in EEC and other syndromes. *J. Med. Genet.* **39**, 377–381 (2002).
9. G. Pellegrini *et al*., p63 identifies keratinocyte stem cells. *Proc. Natl. Acad. Sci. U.S.A.* **98**, 3156–3161 (2001).
10. A. B. Truong, P. A. Khavari, Control of keratinocyte proliferation and differentiation by p63. *Cell Cycle* **6**, 295–299 (2007).
11. D. K. Carroll, J. S. Brugge, L. D. Attardi, p63, cell adhesion and survival. *Cell Cycle* **6**, 255–261 (2007).
12. S. Wolff *et al*., The alpha/beta carboxy-terminal domains of p63 are required for skin and limb development. New insights from the Brdm2 mouse which is not a complete p63 knockout but expresses p63 gamma-like proteins. *Cell Death Differ.* **16**, 1108–1117 (2009).
13. D. Chakravarti *et al*., Induced multipotency in adult keratinocytes through down-regulation of ΔNp63 or DGCR8. *Proc. Natl. Acad. Sci. U.S.A.* **111**, E572–E581 (2014).
14. R. Shalom-Feuerstein *et al*., ΔNp63 is an ectodermal gatekeeper of epidermal morphogenesis. *Cell Death Differ.* **18**, 887–896 (2011).
15. C. Trapnell *et al*., The dynamics and regulators of cell fate decisions are revealed by pseudotemporal ordering of single cells. *Nat. Biotechnol.* **32**, 381–386 (2014).
16. A. Olsson *et al*., Single-cell analysis of mixed-lineage states leading to a binary cell fate choice. *Nature* **537**, 698–702 (2016).
17. S. Yamanaka, H. M. Blau, Nuclear reprogramming to a pluripotent state by three approaches. *Nature* **465**, 704–712 (2010).
18. R. Shalom-Feuerstein *et al*., Impaired epithelial differentiation of induced pluripotent stem cells from ectodermal dysplasia-related patients is rescued by the small compound APR-246/PRIMA-1MET. *Proc. Natl. Acad. Sci. U.S.A.* **110**, 2152–2156 (2013).
19. J. A. Thomson *et al*., Embryonic stem cell lines derived from human blastocysts. *Science* **282**, 1145–1147 (1998).
20. M. Itoh, M. Kiuru, M. S. Cairo, A. M. Christiano, Generation of keratinocytes from normal and recessive dystrophic epidermolysis bullosa-induced pluripotent stem cells. *Proc. Natl. Acad. Sci. U.S.A.* **108**, 8797–8802 (2011).
21. X. Fan *et al*., Single cell and open chromatin analysis reveals molecular origin of epidermal cells of the skin. *Dev. Cell* **47**, 21–37.e5 (2018).
22. J. M. Pattison *et al*., Retinoic acid and BMP4 cooperate with p63 to alter chromatin dynamics during surface epithelial commitment. *Nat. Genet.* **50**, 1658–1665 (2018).
23. L. Li *et al*., TFAP2C- and p63-dependent networks sequentially rearrange chromatin landscapes to drive human epidermal lineage commitment. *Cell Stem Cell* **24**, 271–284.e8 (2019).
24. S. Islam *et al*., Highly multiplexed and strand-specific single-cell RNA 5′ end sequencing. *Nat. Protoc.* **7**, 813–828 (2012).
25. D. Risso, J. Ngai, T. P. Speed, S. Dudoit, Normalization of RNA-seq data using factor analysis of control genes or samples. *Nat. Biotechnol.* **32**, 896–902 (2014).
26. J. Tchieu *et al*., A modular platform for differentiation of human PSCs into all major ectodermal lineages. *Cell Stem Cell* **21**, 399–410.e7 (2017).
27. M. Michaelis *et al*., Valproic acid inhibits angiogenesis in vitro and in vivo. *Mol. Pharmacol.* **65**, 520–527 (2004).
28. M. Wei *et al*., Valproic acid sensitizes metformin-resistant human renal cell carcinoma cells by upregulating H3 acetylation and EMT reversal. *BMC Cancer* **18**, 434 (2018).
29. P. Cardellini, C. Polo, S. Coral, Suramin and heparin: Aspecific inhibitors of mesoderm induction in the Xenopus laevis embryo. *Mech. Dev.* **45**, 73–87 (1994).
30. C. E. Friedman *et al*., Single-cell transcriptomic analysis of cardiac differentiation from human PSCs reveals HOPX-dependent cardiomyocyte maturation. *Cell Stem Cell* **23**, 586–598.e8 (2018).
31. N. Forster *et al*., Basal cell signaling by p63 controls luminal progenitor function and lactation via NRG1. *Dev. Cell* **28**, 147–160 (2014).
32. J. Shen *et al*., APR-246/PRIMA-1(MET) rescues epidermal differentiation in skin keratinocytes derived from EEC syndrome patients with p63 mutations. *Proc. Natl. Acad. Sci. U.S.A.* **110**, 2157–2162 (2013).
33. I. Pastushenko *et al*., Identification of the tumour transition states occurring during EMT. *Nature* **556**, 463–468 (2018).
34. A. Friedl, Z. Chang, A. Tierney, A. C. Rapraeger, Differential binding of fibroblast growth factor-2 and -7 to basement membrane heparan sulfate: Comparison of normal and abnormal human tissues. *Am. J. Pathol.* **150**, 1443–1455 (1997).
35. A. Singh Grewal, D. Pandita, S. Bhardwaj, V. Lather, Recent updates on development of drug molecules for human African trypanosomiasis. *Curr. Top. Med. Chem.* **16**, 2245–2265 (2016).
36. N. Wakayama, T. Katow, H. Katow, Characterization and endocytic internalization of epith-2 cell surface glycoprotein during the epithelial-to-mesenchymal transition in sea urchin embryos. *Front. Endocrinol.* **4**, 112 (2013).
37. J. Waltenberger, U. Mayr, H. Frank, V. Hombach, Suramin is a potent inhibitor of vascular endothelial growth factor. A contribution to the molecular basis of its antiangiogenic action. *J. Mol. Cell. Cardiol.* **28**, 1523–1529 (1996).
38. Z. S. Wu, C. F. Liu, B. Fu, R. H. Chou, C. Yu, Suramin blocks interaction between human FGF1 and FGFR2 D2 domain and reduces downstream signaling activity. *Biochem. Biophys. Res. Commun.* **477**, 861–867 (2016).
39. S. Zhuang, R. G. Schnellmann, Suramin promotes proliferation and scattering of renal epithelial cells. *J. Pharmacol. Exp. Ther.* **314**, 383–390 (2005).
40. M. Lopez-Perez, E. P. Salazar, A role for the cytoskeleton in STAT5 activation in MCF7 human breast cancer cells stimulated with EGF. *Int. J. Biochem. Cell Biol.* **38**, 1716–1728 (2006).
41. S. Donnini *et al*., EGFR signaling upregulates expression of microsomal prostaglandin E synthase-1 in cancer cells leading to enhanced tumorigenicity. *Oncogene* **31**, 3457–3466 (2012).
42. B. Orzechowska, J. Pabijan, J. Wiltowska-Zuber, J. Zemła, M. Lekka, Fibroblasts change spreading capability and mechanical properties in a direct interaction with keratinocytes in conditions mimicking wound healing. *J. Biomech.* **74**, 134–142 (2018).
43. E. Warlich *et al*., Lentiviral vector design and imaging approaches to visualize the early stages of cellular reprogramming. *Mol. Ther.* **19**, 782–789 (2011).